



ISSN 1110-0451

Web site: ajnsa.journals.ekb.eg



(E S N S A)

Capability of Mathematical Probability Tables to Treat Resonance Interference among Isotopes

Basma FOAD^{1,2}

⁽¹⁾ McMaster University, 1280 Main Street West, Hamilton, Ontario, L8S 4L7, Canada.

⁽²⁾ Egypt Nuclear and Radiological Regulatory Authority, 3 Ahmad El Zomar St., Nasr City, Cairo, 11787, Egypt.

ARTICLE INFO

Article history:

Received: 27th Mar. 2021

Accepted: 4th Aug. 2022

Keywords:

Self-shielding effect,
Resonance overlapping,
Subgroup method,
Mathematical probability
tables,
PWR.

ABSTRACT

In light water reactors, it is very important to consider the resonance self-shielding behavior of the cross-section, where the accuracy of the calculation method is related to the technique used to represent the self-shielding distribution. The impact of the self-shielding on one nuclide cross-section can depend strongly on the resonance cross-section of other nuclides in the composition, accordingly, the mutual resonance interference between different resonance isotopes should be considered. The advanced subgroup technique based on the mathematical probability tables can treat such effect, where the Ribon extended model (RIB) and the subgroup projection method (SPM) are available in DRAGON4 code. The calculations are performed for three PWR fuel types namely, UO₂, ThO₂-UO₂, and PuO₂-UO₂, and the obtained results are benchmarked with the reference MCNP6 calculations. The main purpose of these studies is to investigate which isotope can be included in the correlation model and the results indicate that the contribution of some isotopes may disturb other cross-sections leading to deviation from MCNP results. Consequently, those isotopes should be removed from the correlation model especially for the PuO₂-UO₂ fuel pin.

1. INTRODUCTION

The fundamental problem for any resonance self-shielding method is that the method treats each resonant isotope as if it is isolated, i.e. the isotopes are treated as if there are no other isotopes with resonances present in the material. In reality, the cross-sections belonging to energy group g may include many resonances, where cross-sections and fluxes exhibit resonant behavior with peaks and minima in opposite directions. Furthermore, resonances from other isotopes can also cause the fluxes to exhibit minima. When resonances from different isotopes are overlapping then the mutual resonance self-shielding interference occurs. For example, in PWR-MOX (PuO₂-UO₂) fuel, there is interference between the 20.9 eV resonance of ²³⁸U and the 20.45 eV resonance of ²⁴⁰Pu in addition to the interference between the 66.0 eV resonance of ²³⁸U and the 66.2 eV resonance of ²⁴⁰Pu [1].

In recent years, there are challenges to improve the self-shielding models in deterministic codes by

considering the mutual self-shielding of overlapping resonances between different resonance isotopes [2]. An advanced correction model is introduced to effectively represent such effect based on the subgroup method using mathematical probability tables. Typically, the Ribon extended model (RIB) and the subgroup projection method (SPM) are applied, where the mathematical probability table is generated using the CALENDF approach [3].

In our previous work [4], various self-shielding models were investigated using DRAGON [5] and WIMS-D5 codes [6], where the results were compared to the MCNP6 as a reference code [7]. The results indicated that DRAGON4 code, using both physical or mathematical probability tables, gives a better representation of self-shielding phenomena. However, the mutual self-shielding due to resonance interference effects between different resonant isotopes have been neglected in the present work.

In the current study, the advantages and drawbacks of the correlated weight matrices used to represent the interferences among different isotopes will be discussed. The correlation existing between different cross-section sets of a unique isotope present in regions having different temperatures will not be considered. Consequently, the temperatures are assumed to be uniform within the fuel rod to avoid the temperature correlation.

The calculations are computed using DRAGON4 code [5] based on RIB and SPM approaches for representing the resonance self-shielding. However, the accuracy of both techniques has been investigated by comparing the results with those of the Monte Carlo MCNP6 code [7].

Three types of PWR fuel cells will be analyzed namely, the UO₂, and Th-MOX (ThO₂-UO₂), and Pu-MOX (PuO₂-UO₂) fueled cells. The pin cell model description is presented in a previous work[4]. The resonance interference model is described in section 2 and the numerical results are explained in section 3.

2. The Interference Correlation Model

The resonance self-shielding calculation is necessary for any deterministic code to solve the neutron transport equation [8]. The equivalence in dilution approach [9] and subgroup method [10] are widely used to represent the resonant behavior of the cross-section in each energy group. The results of our previous work [4] indicated that the subgroup method based on both physical and mathematical probability tables, gives a better representation of self-shielding phenomena.

In the physical probability tables, the resonance integral (RI) tables are converted into a set of subgroup levels and weights by preserving the RI or effective cross-section over different background cross-sections [11]. However, the correlated weights matrices, which represent the effect of resonance overlapping of one isotope on the absorption of another isotope that has a resonance at the same energy, cannot be computed[12].

The mathematical probability tables approach is an extension of the CALENDF formalism [3], where the mathematical probability tables are computed in such a way as to preserve the selected moments of the resonant cross-sections instead of preserving the RI or effective cross-section. The presented study focuses on the mathematical probability tables approach which can

treat the interference effects between resonance isotopes, more details will be explained in the next section. More details about the subgroup method are available in a previous work[4].

A new correlation model is introduced to represent interference effects between resonances isotopes. The conditional probability density $\Pi(\sigma^a, \sigma^b)$ in group g is defined in such a way that $\Pi(\sigma^a, \sigma^b)d\sigma^a d\sigma^b$ is equal to the probability for the total cross-section of isotope a to have a value between σ^a and $\sigma^a + d\sigma^a$ and for the total cross-section of isotope b to have a value between σ^b and $\sigma^b + d\sigma^b$ [13]. Accordingly, any Riemann integral in lethargy can be replaced by an equivalent Lebesgue integral.

$$\frac{1}{\Delta u_g} \int_{u_{g-1}}^{u_g} du f[\sigma^a(u), \sigma^b(u)] = \int_0^{\max(\sigma^a)} d\sigma^a \int_0^{\max(\sigma^b)} d\sigma^b \Pi(\sigma^a, \sigma^b) \times f(\sigma^a, \sigma^b) \quad (4)$$

Where the conditional probability density can be written in terms of the two-isotopes correlated weight matrix $\omega_{k,l}^{ab}$ defined as follows:

$$\Pi(\sigma^a, \sigma^b) = \sum_{k=1}^K \sum_{l=1}^L \delta(\sigma^a - \sigma_k^a) \delta(\sigma^b - \sigma_l^b) \omega_{k,l}^{ab} \quad (5)$$

Where K and L are the order of the probability tables for isotopes a and b , respectively. The corresponding discretization of Riemann integral in lethargy is obtained by substitution of Eq. (5) into Eq. (4) as follows:

$$\frac{1}{\Delta u_g} \int_{u_{g-1}}^{u_g} du f[\sigma^a(u), \sigma^b(u)] = \sum_{k=1}^K \sum_{l=1}^L \omega_{k,l}^{ab} f(\sigma_k^a, \sigma_l^b) \quad (6)$$

The two-isotopes correlated weight matrix is normalized in such a way that

$$\sum_{k=1}^K \omega_{k,l}^{ab} = \omega_l^b \text{ and } \sum_{l=1}^L \omega_{k,l}^{ab} = \omega_k^a$$

Where ω_k^a and ω_l^b are the weights corresponding to cross-sections $\sigma^a(u)$ and $\sigma^b(u)$, respectively. The correlated weight matrix $\omega_{k,l}^{ab}$ can be computed using a CALENDF approach. In general, there are two models based on the mathematical probability tables and have the capabilities to treat the interference effects between resonance isotopes: the Ribon extended model and the subgroup projection method.

1. The Ribon extended model (RIB): The slowing-down effect in the resolved energy domain is represented by correlated 2-D probability tables, where the elastic slowing-down kernel is described by a term in $e^{u-u'}$. This term creates a slowing-down correlation in probability tables. This correlation vanishes at high energy (above 10 keV) or if the energy mesh is fine [1]. Although the RIB can be used to represent the mutual shielding effect between different isotopes, it is not sufficiently accurate to represent the temperature gradient in a fuel rod.
2. The subgroup projection method (SPM): The Ribon extended model is simplified by removing the slowing down correlation mode using a large numbers of fine energy mesh in the slowing-down range [14]. The SPM approach has developed a new cross-section correlation model (based on CALENDF mathematical probability table) with the capability to represent the temperature gradient effects in fuel [15].

3. Numerical Results

The PWR fuel rod is divided into six rings so that the spatial resonance self-shielding distribution can be observed which affects the build-up of plutonium near the fuel surface (rim effect) [16]. The nuclear data libraries used by DRAGON4 and MCNP6 codes are based on the ENDF/B-VII.1 cross-section data library, where the DRAG libraries, XMAS-172 and SHEM-281 energy group, are used with RIB (PTSL PTSL keyword to enable the calculation of CALENDF-type probability tables, consistent with the Ribon extended model, in some energy groups [5]). The SHEM-295 and SHEM-361 DRAG libraries are used with the SPM approach (PT keyword to activate the calculation of the CALENDF-type mathematical probability tables, without slowing-down correlated weight matrices, using the bin-type cross-section data as input. This option is compatible with the Sanchez-Coste self-shielding method and with the subgroup projection method (SPM) [5]), where the energy widths in the resolved energy domain are too small.

Table (1) shows a comparison of k_{inf} obtained with DRAGON4 code using both RIB and SPM approaches with MCNP6 for the UO₂ pin cell. There are good agreements between DRAGON4 results and those of

MCNP6 if the correlation between the isotopes is neglected. The SPM associated with the SHEM-295 library gives the best results since $|\Delta k/k|$ is 21 pcm. Both RIB and SPM could not improve the results when the interference between ²³⁸U and ²³⁵U is considered, ($|\Delta k/k|$ is unchanged or becomes larger).

Table (1): The k_{inf} results for UO₂ fuel

Self-shielding model	Library	Correlated isotopes	k_{inf}	$\Delta k/k$
MCNP6	ENDF/B-VII.1	-	1.40780	\mp 22 pcm
Ribon extended model (RIB)	XMAS-172	-	1.40684	68
		²³⁸ U, ²³⁵ U	1.40684	68
	SHEM-281	-	1.40681	70
		²³⁸ U, ²³⁵ U	1.40587	137
Subgroup projection method (SPM)	SHEM-295	-	1.40750	21
		²³⁸ U, ²³⁵ U	1.40699	57
	SHEM-361	-	1.40733	33
		²³⁸ U, ²³⁵ U	1.40732	34

The ²³⁵U fission and ²³⁸U capture rates for the UO₂ fuel pin are presented in Figures (1 and 2) respectively. It can be seen that both reaction rates are very close to MCNP6 results with and without considering the interference between ²³⁸U and ²³⁵U. Although the XMAS-172 library uses fewer energy groups compared to SHEM libraries, it succeeds to represent the k_{inf} and the radial distribution of the reaction rates, thanks to the slowing-down correlation matrix that exists in the Ribon extended model.

For the Th-MOX fuel type, the results are not good as those obtained for UO₂ where all the values of $|\Delta k/k|$ are greater than 100 pcm as shown in Table (2). The RIB results are better when the correlation between the isotopes is neglected (especially if ²³²Th is not involved in the correlation). It seems that both XMAS-172 and SHEM-281 libraries do not consider the resonances of ²³²Th. The values of k_{inf} get closer to MCNP6 if the SPM is used, and $|\Delta k/k|$ is reduced to 102 pcm when the interference between the three resonance isotopes is considered (²³⁸U, ²³⁵U, and ²³²Th).

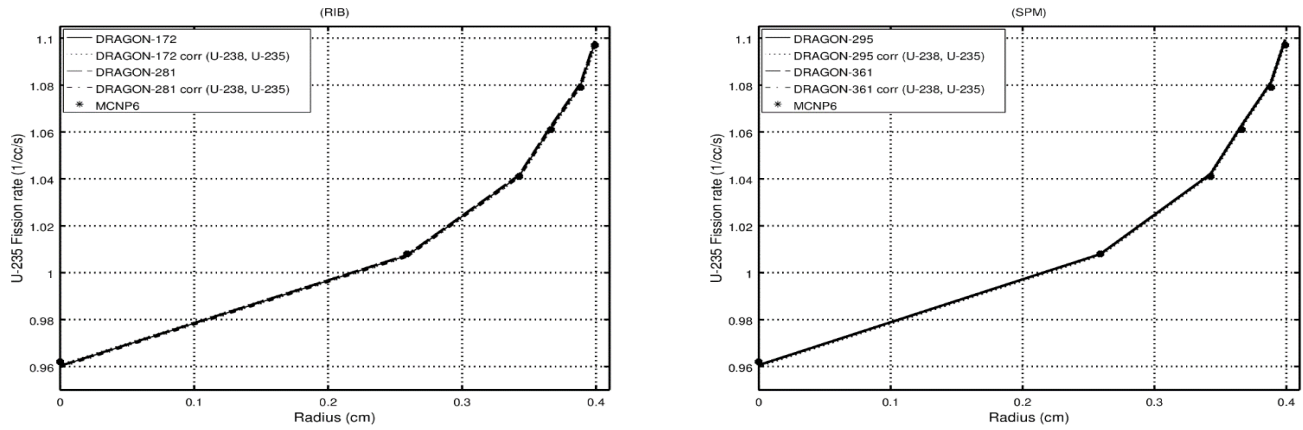


Fig. (1): ^{235}U fission rate radial distribution in UO_2

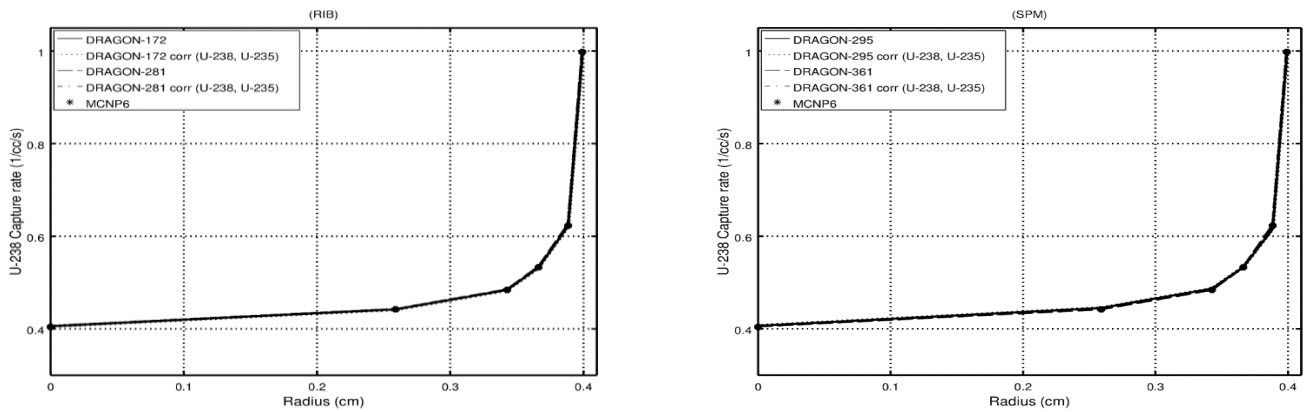


Fig. (2): ^{238}U capture rate radial distribution in UO_2

Table (2): The k_{inf} results for Th-MOX fuel

Self-shielding model	Library	Correlated isotopes	k_{inf}	$\Delta k/k$
MCNP6	ENDF/B-VII.1	-	1.30764 \mp 21 pcm	-
Ribon extended model	XMAS-172	-	1.30349	317
		^{238}U , ^{235}U	1.30336	327
		^{238}U , ^{232}Th	1.30031	561
	(RIB)	^{238}U , ^{235}U , ^{232}Th	1.30032	560
		-	1.30367	304
		^{238}U , ^{235}U	1.30321	339
Subgroup projection method	SHEM-281	^{238}U , ^{232}Th	1.29883	674
		^{238}U , ^{235}U , ^{232}Th	1.29815	726
		-	1.30531	178
	(SPM)	^{238}U , ^{235}U	1.30520	187
		^{238}U , ^{232}Th	1.30440	-248
		^{238}U , ^{235}U , ^{232}Th	1.30560	156
SHEM-361	-	1.30536	174	
	^{238}U , ^{235}U	1.30535	175	
	^{238}U , ^{232}Th	1.30489	210	
		^{238}U , ^{235}U , ^{232}Th	1.30630	102

The ²³²Th capture rates are indicated in Figure (3), where there are agreements with MCNP6 results. As previously mentioned, there is a small deviation in the results using RIB if ²³²Th is involved in the correlation model (particularly, results associated with the SHEM-281 library).

For the Pu-MOX pin cell, the contributions of some isotopes may disturb other cross-sections leading to

discrepancy from MCNP6 results as indicated in Table(3). Considering ²³⁸U and ²⁴⁰Pu in the RIB correlation model reduces $|\Delta k/k|$ to about 1 pcm, even though including all resonance isotopes in the RIB correlation leads to discrepancy from MCNP6 and $|\Delta k/k|$ reaches 4871 and 16610 pcm for XMAS-172 and SHEM-281 libraries, respectively

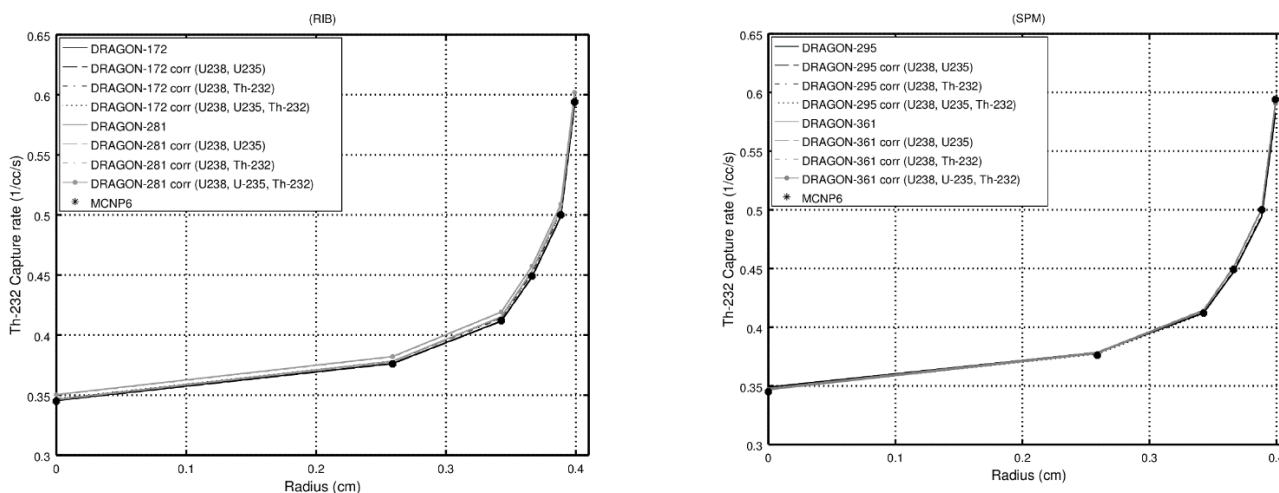


Fig. (3): ²³²Th capture rate radial distribution in Th-MOX pin

Table (3): The k_{inf} results for Pu-MOX fuel

Self-shielding model	Library	Correlated isotopes	k_{inf}	$\Delta k/k$	
MCNP6	ENDF/B-VII.1	-	1.156747 ± 22 pcm	-	
Ribon extended model	XMAS-172	-	1.15401	236	
		²³⁸ U, ²⁴⁰ Pu	1.15672	2	
		²³⁸ U, ²⁴⁰ Pu, ²³⁹ Pu	1.15737	-54	
	(RIB)	SHEM-281	All resonance isotopes	1.21308	4871
			-	1.15554	104
			²³⁸ U, ²⁴⁰ Pu	1.15673	1
Subgroup projection method	SHEM-295	²³⁸ U, ²⁴⁰ Pu, ²³⁹ Pu	1.15706	-28	
		All resonance isotopes	1.34887	-16610	
		-	1.15617	49	
	(SPM)	SHEM-361	²³⁸ U, ²⁴⁰ Pu	1.15606	59
			²³⁸ U, ²⁴⁰ Pu, ²³⁹ Pu	1.15644	26
			All resonance isotopes	1.15636	33
-	-	1.15682	-7		
²³⁸ U, ²⁴⁰ Pu	1.15642	28			
²³⁸ U, ²⁴⁰ Pu, ²³⁹ Pu	1.15677	-2			
All resonance isotopes	1.15678	-3			

However, including all isotopes in the SPM correlation model improves the values of k_{inf} and the best results are obtained if the interference of the three ^{238}U , ^{239}Pu , and ^{240}Pu isotopes is only considered, where $|\Delta k/k|$ is reduced to 2 pcm

using the SHEM-361 library. To investigate the reason which causes these divergences in the Pu-MOX fuel cell, the ^{239}Pu fission, and ^{239}Pu , ^{240}Pu , and ^{238}U capture rates are presented in Figures (4 _ 7)

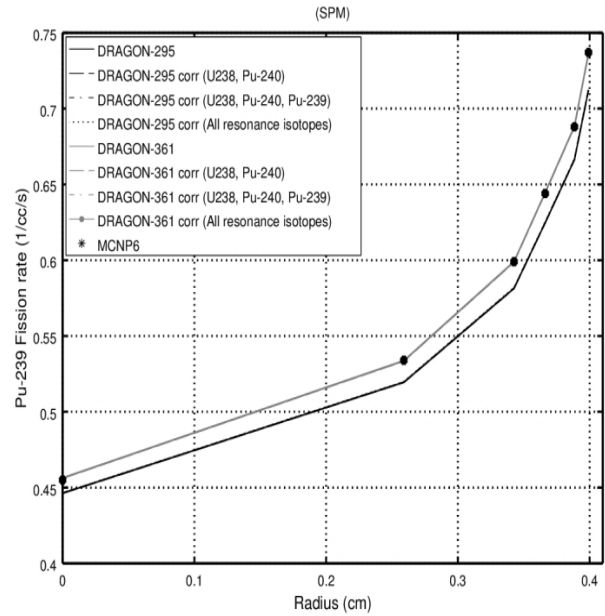
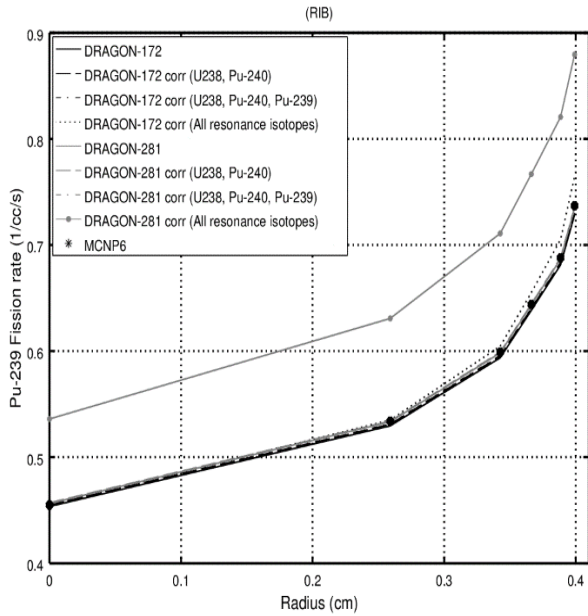


Fig. (4): ^{239}Pu fission rate radial distribution in Pu-MOX pin

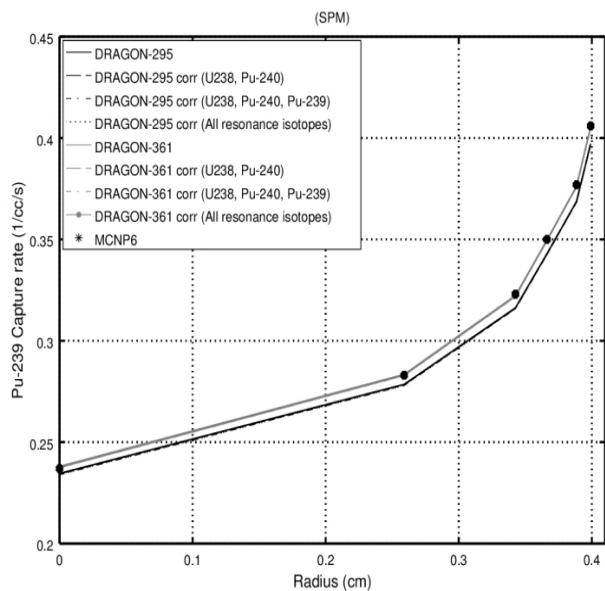
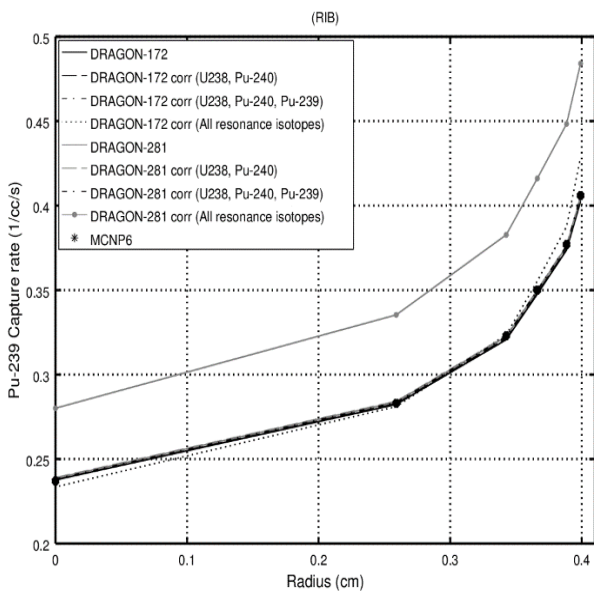


Fig. (5): ^{239}Pu capture rate radial distribution in Pu-MOX pin

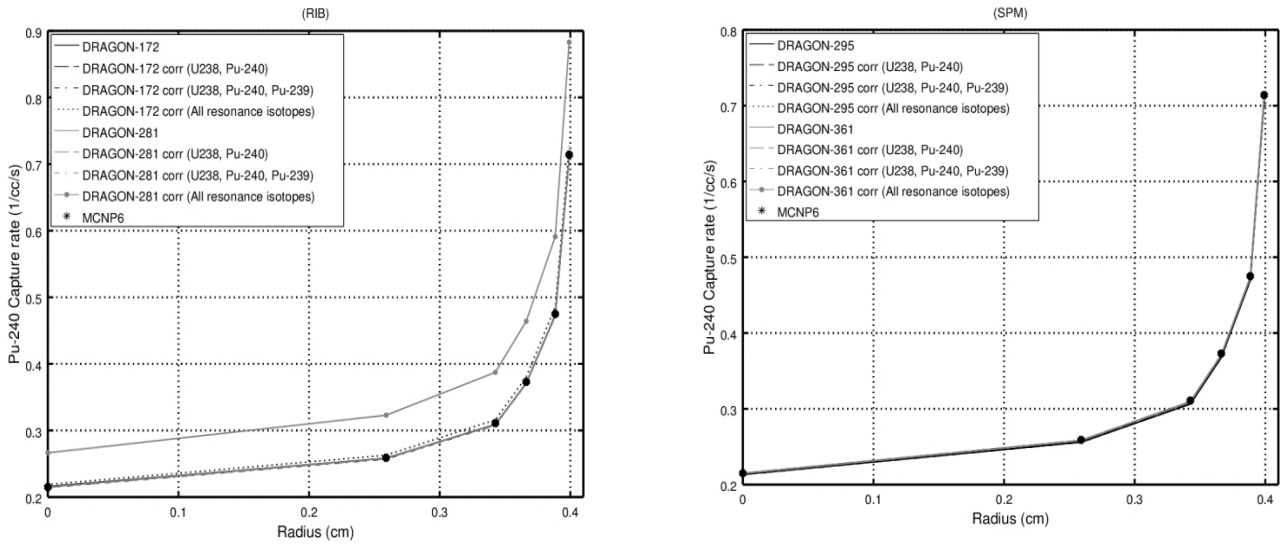


Fig. (6): ²⁴⁰Pu capture rate radial distribution in Pu-MOX pin

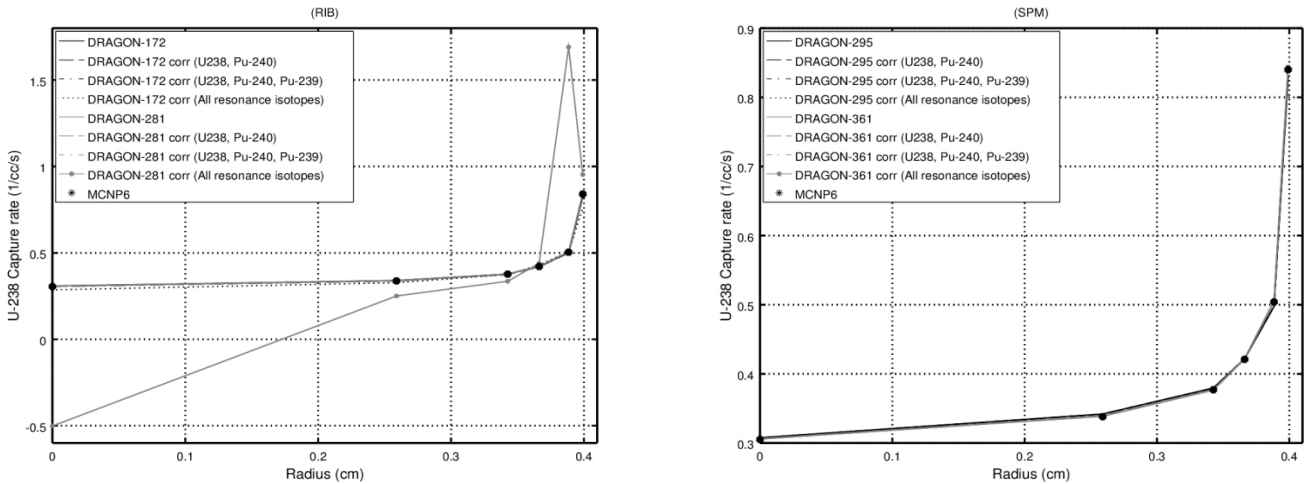


Fig. (7): ²³⁸U capture rate radial distribution in Pu-MOX pin

For the RIB approach, the ²³⁹Pu fission and capture rates in addition to ²⁴⁰Pu capture rates are almost similar to MCNP6 except for results associated with SHEM-281 if all resonance isotopes are involved in the correlation model. These deviations are due to the slowing-down correlation model used in RIB which affects the flux as shown in Figure (8).

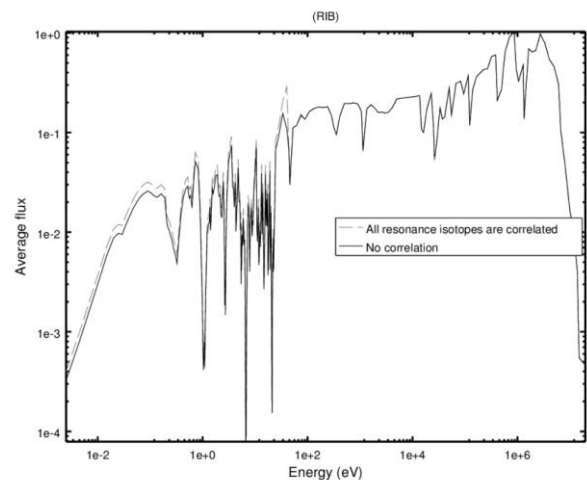


Fig. (8): Average flux in Pu-MOX pin using SHEM-281 library

For the SPM approach, the ^{239}Pu fission and capture, and ^{240}Pu capture rates calculated using the SHEM-361 library are in a good agreement with MCNP6 results, this is because a finer energy mesh, using as many as 361 energy groups, is permitting a better representation of self-shielding phenomena in the resonance energy domain.

The behavior of ^{238}U capture rates associated with the SHEM-281 library is very complicated when considering all resonance isotopes in the RIB correlation model. There is a large divergence in the results especially in the inner and outer regions (in opposite directions). To understand the reason causing these discrepancies, the ^{238}U energy group cross-sections for the SHEM-281 library calculated using RIB are explained in Figure (9), when all resonance isotopes are correlated.

The ^{238}U cross-sections have the normal profile except the resonance around 40 eV, there is an overestimate of the cross-section in regions 5 and 6. To see this deviation in more detail, the cross-sections around this energy group are plotted using a non-logarithmic scale to show both positive and negative values. It is found that in the

90th energy group of SHEM-281 library (33.7 ~ 40.2 eV) there are huge differences in the ^{238}U capture cross-sections which cause discrepancies of ^{238}U capture rates.

To fully understand the reason for these deviations and realize why those discrepancies are significant for SHEM-281; Figure (10) reveals that every library (XMAS-172, SHEM-281, and SHEM-361) has a different energy structure (group energy boundary).

Although XMAS-172 has fewer energy groups, the energy domain 33.7 ~ 40.2 eV is divided into two energy groups (33.7 ~ 37.27 eV and 37.27 ~ 40.2 eV) while SHEM-281 has only one energy group. Particularly, this energy domain contains many resonances (^{238}U , ^{239}Pu , ^{240}Pu , ...etc.), and considering the interference of all resonance isotopes in the correlation model may disturb the model leading to these deviations. Using the optimized SHEM-361 library gives the best results because its energy structure permits a better representation of self-shielding phenomena between 22.5 eV and 11.14 keV (especially ^{238}U cross-section structure).

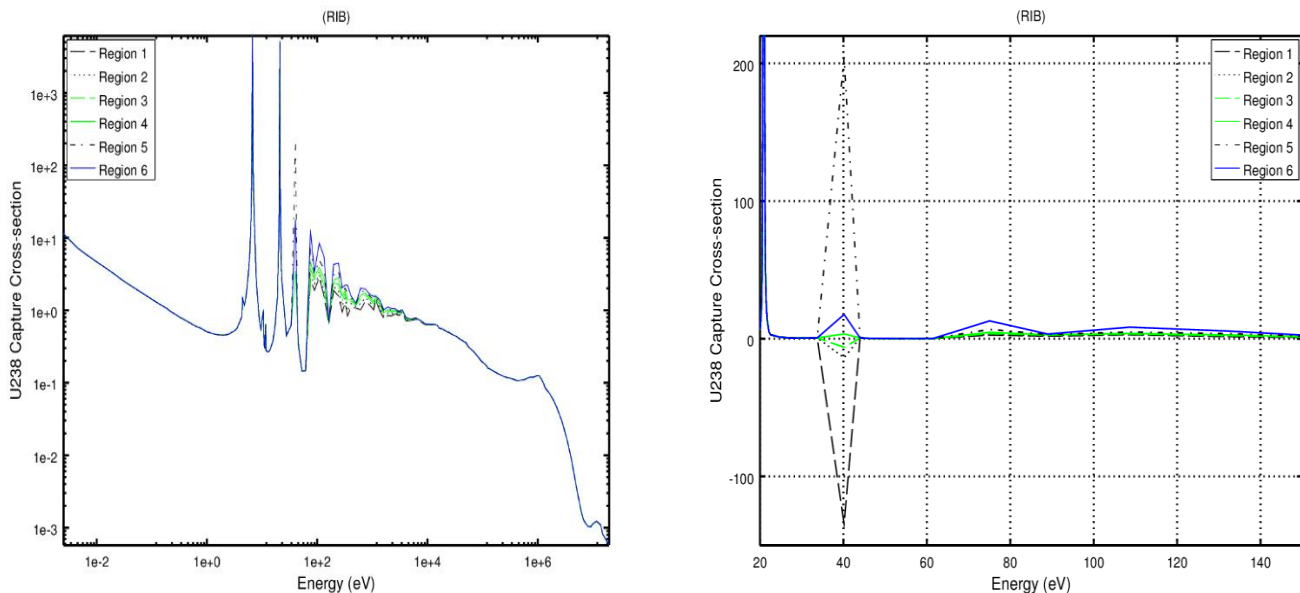


Fig. (9): ^{238}U capture cross-section for SHEM-281 library when all resonance isotopes are correlated in Pu-MOX pin

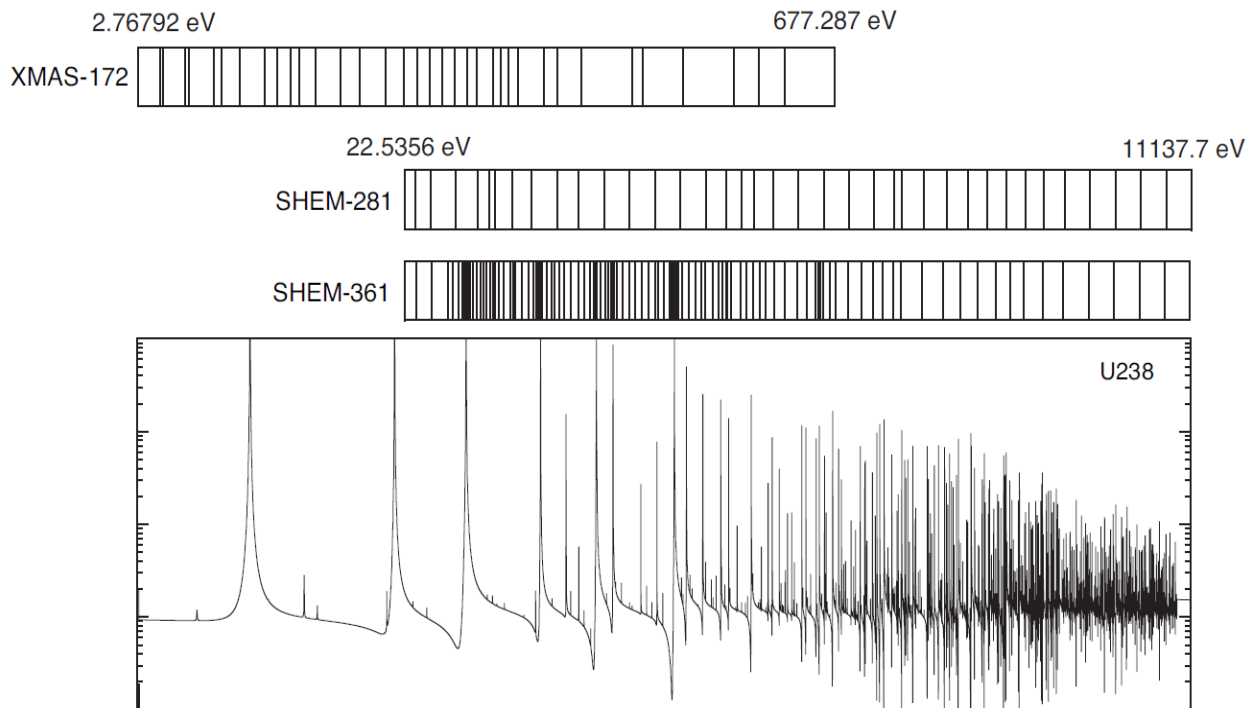


Fig. (10): ^{238}U resonances and energy groups in the resolved energy domain for XMAS-172, SHEM-281, and SHEM-361 libraries

4. CONCLUSION

In the present study, the subgroup method based on the mathematical probability tables is used to represent the self-shielding interference among resonance isotopes and the accuracy of the calculations is performed by comparing the results with MCNP6 for three different fuel types. The lattice calculations were performed using a developed version of DRAGON code based on Ribon extended model (RIB) and the subgroup projection method (SPM), where a new correlated matrix, which is calculated internally by the code, is introduced to represent such interference effects. Although both methods can predict the correct k_{inf} and radial reaction rates distribution, the existence of some resonance isotopes in the correlation model may disturb the cross-sections of other isotopes. For the $\text{PuO}_2\text{-UO}_2$ fuel pin, there are large discrepancies from MCNP6 results when all resonance isotopes are considered in the correlation, and $|\Delta k/k|$ reaches 16610 pcm for SHEM-281 library. The best result is achieved when using the SPM approach associated with the SHEM-361 library due to its optimized fine mesh structure, where $|\Delta k/k|$ are reduced to 34, 102, and 2 pcm for UO_2 , $\text{ThO}_2\text{-UO}_2$, and $\text{PuO}_2\text{-UO}_2$ fuel pins, respectively.

REFERENCES

- [1] Hebert, A., 2004. A Mutual Resonance Shielding Model Consistent with Ribon Subgroup Equations. PHYSOR Chicago, IL.
- [2] Liu, Y., and Martin, W. R., 2017. Pin-resolved Resonance Self-shielding Methods in LWR Direct Transport Calculations. *Annals of Nuclear Energy*, 110 (1165–1175).
- [3] Ribon, P., 1989. Statistical Probability Tables. CALENDF Program., Proc. of the Seminar on NJOY and THEMIS. Saclay, France, June 20-21, 1989, p.220 . 232, OECD/NEA Data Bank.
- [4] Foad B. and Refeat R., 2018. Estimation of resonance self-shielding effect in PWR pin cell for different fuel types. *Annals of Nuclear Energy*, 120, 805-813.
- [5] Marleau, G., Hebert, A., and Roy, R., 2013. A User Guide for DRAGON Version4, IGE–294.
- [6] NEA, 1997. WIMSD: A Neutronics Code for Standard Lattice Physics Analysis. NEA-1507/04, Answers Software Service, AEA Technology.

- [7] Pelowitz, D. B. , 2013. MCNP6 User's Manual. LA-CP-13-00634, Rev.0.
- [8] Cacuci, D. G., 2010. Handbook of Nuclear Engineering. Springer.
- [9] Choia, S., and Lee, D., 2016. Improved Resonance Self-shielding Method Considering Resonance Scattering Effect. PHYSOR 2016, Sun Valley, ID.
- [10] Martin, N. and Hebert, A., 2009. Application of Advanced Self-shielding Models to Criticality-Safety Studies. International Conference on Mathematics, Computational Methods, and Reactor Physics.
- [11] Qingming, He., et al, 2017. Treatment of Nonuniform Temperature Distribution by Subgroup Method. Transactions of the American Nuclear Society, Vol. 116, San Francisco, California, June 11–15.
- [12] Hebert, A., 2007. A Review of Legacy and Advanced Self-Shielding Models for Lattice Calculations. Nuclear science and engineering, Volume 155, Issue 2.
- [13] Hebert, A., 2005. The Ribon Extended Self-shielding Model. Nuclear science and engineering, Volume 151, 1–24.
- [14] Hebert, A. , 2009. Applied Reactor Physics. Presses inter Poly technique.
- [15] Hebert, A., 2014. Representations of the Temperature Correlation Effect in Lattice Calculations. Review of Applied Physics, Volume3.
- [16] Reuss, P., 2008. Neutron Physics. EDP Sciences.